RAPID COMMUNICATIONS

PHYSICAL REVIEW C

NUCLEAR PHYSICS

THIRD SERIES, VOLUME 47, NUMBER 6 JUNE 1993

## RAPID COMMUNICATIONS

*The Rapid Communications section is intended for the accelerated publication of important new results. Manuscripts submitted to this section are given priority in handling in the editorial office and in production. A Rapid Communication in* **Physical Review C** *may be no longer than five printed pages and must be accompanied by an abstract. Page proofs are sent to authors.*

# Neutron decay of $^{10}$Li produced by fragmentation

R. A. Kryger,[1] A. Azhari,[1,2] A. Galonsky,[1,2] J. H. Kelley,[1,2] R. Pfaff,[1,2] E. Ramakrishnan,[1,2] D. Sackett,[1,2]* B. M. Sherrill,[1,2] M. Thoennessen,[1,2] J. A. Winger,[1] and S. Yokoyama[1,2]

[1] *National Superconducting Cyclotron Laboratory, Michigan State University, East Lansing, Michigan 48824*

[2] *Department of Physics and Astronomy, Michigan State University, East Lansing, Michigan 48824*

(Received 16 February 1993)

The neutron decay of $^{10}$Li, produced in the reaction of 80 MeV/nucleon $^{18}$O + $^{nat}$C, was studied by the coincidence detection of neutrons and $^{9}$Li nuclei in a collinear geometry. An analysis of the relative velocity spectrum indicates the presence of a $^{10}$Li state which decays by very low energy neutron emission. This state corresponds to either the ground state of $^{10}$Li, in which case it is probably an $s$-wave resonance, or an excited state at $E_x \approx 2.5$ MeV.

PACS number(s): 27.20.+n, 21.10.Dr

The experimental study of the structure of very neutron- and proton-rich nuclei provides new insight into the properties of nuclear matter and unique tests for nuclear models. This is true not only for the long-lived radioactive nuclei that undergo $\beta$ decay, but also for the particle-unstable nuclei just beyond the driplines. Experimental investigations of these latter nuclei are usually difficult because of very short lifetimes and typically low production cross sections associated with reactions involving stable nuclear beams and targets. One particularly interesting case is the neutron-unbound nucleus $^{10}$Li because of its importance to the understanding of the halo nucleus $^{11}$Li. The present uncertainty concerning the $n$+$^{9}$Li potential results in significant limitations on the ability of three-body models of the $^{11}$Li system to account for the two-neutron separation energy and to predict the two-neutron relative wave function [1, 2]. Unfortunately, there is little data available regarding the $^{10}$Li system. Wilcox *et al.* [3] published the first measurement of the mass of $^{10}$Li using the reaction $^{9}$Be($^{9}$Be,$^{8}$B)$^{10}$Li. They reported a mass excess for $^{10}$Li of $\Delta = 33.83 \pm 0.25$ MeV, corresponding to a neutron separation energy of $S_n = 0.80 \pm 0.25$ MeV and a width of $\Gamma = 1.2 \pm 0.3$ MeV. A second study by Amelin *et al.* [4] involved the reaction $^{11}$B($\pi^-, p$)$^{10}$Li and reported a $^{10}$Li separation energy of $S_n = 0.15 \pm 0.15$ MeV and a width of $\Gamma < 0.4$ MeV. Very recently, measurements by Bohlen *et al.* [5] and Young [6] confirm the existence of one (or more) state(s) in the $^{10}$Li system with separation energies between 400 and 800 keV. However, the existence of a lower lying state remains unconfirmed.

We have applied the technique of sequential neutron decay spectroscopy [7] (SNDS) to fragmentation reaction products produced near 0° in order to investigate the structure of light nuclei beyond the neutron dripline. The SNDS method detects collinear neutron-fragment coincidences from the decay of neutron unbound states. The decay energy $E$ of the parent state is related to the relative velocity $v_{\rm rel}$ of the neutron and fragment by means of the (nonrelativistic) equation $E = \frac{1}{2}\mu v_{\rm rel}^2$ where $\mu$ is the reduced mass of the neutron and fragment system. By extending this method to fragments produced near

*Present address: Niton Corporation, 74 Loomis St., Bedford, MA 01730.

 

0° we take advantage of kinematic focusing in the intermediate energy fragmentation reaction and significantly increase the yield relative to experiments performed at large angles.

The experiment was performed at the National Superconducting Cyclotron Laboratory using an 80 MeV/nucleon $^{18}$O beam from the K1200 Cyclotron incident upon a 9 mg/cm$^2$ $^{nat}$C target. Reaction products were momentum analyzed by a section of the beam line consisting of two quadrupole magnets followed by a magnetic dipole, used as a magnetic spectrometer. Fragments with a mass-to-charge ratio of 3 were bent to 11° and focused onto a phoswich fragment detector. The primary beam was bent to 14° by the dipole magnet and dumped approximately 10 m downstream behind more than 1 m of concrete shielding. The phoswich fragment detector was a 10.2 cm diameter cylinder consisting of a 3 mm thick NE102A fast plastic layer and a 9.5 cm thick NE115 slow plastic layer. Light output was detected via two phototubes coupled to the back of the detector. Energy loss ($\Delta E$) in the fast plastic and total energy ($E$) were determined by integrating the charge in the phototube output pulses over narrow and wide time gates. The fragment time of flight (TOF) was determined relative to the accelerator rf, and particle identification (both $A$ and $Z$) was accomplished by means of the $\Delta E$, $E$, and TOF signals. The fragment velocity was determined from the TOF and the target-to-detector flight path of 6.0 m. Neutrons were detected directly at 0° in three 6.3 cm diameter by 7.6 cm cylindrical NE-213 or BC501 liquid scintillator detectors placed 5.0 m from the target. The neutron velocity was determined from the neutron TOF, and the timing resolution for both neutron and fragment TOF was 2.1 ns full width at half-maximum (FWHM). Pulse shape discrimination and TOF cuts were used off line to remove the $\gamma$-ray background events. Relative velocity spectra were formed from the coincident neutron-fragment events separately for each fragment isotope, and the spectra were corrected for the random coincidence background. Shadow bar measurements were also made and the scattered neutron background, found to account for less than 5% of the random-corrected coincidence data, was subtracted.

Figure 1 shows the relative velocity spectrum for coincident neutron + $^6$He events which were obtained simultaneously with the $n$ + $^9$Li data. The data show two peaks at $v_{rel} \approx \pm 0.8$ cm/ns superimposed upon a broad background. The peaks correspond to the decay of the known particle-unstable $^7$He ground state ($S_n = 0.45 \pm 0.03$ MeV, $\Gamma = 0.16 \pm 0.03$ MeV [8]), where the neutron is emitted near either 0° or 180° with respect to the incident beam. The source of background neutron-fragment coincidences was undetermined; however, a thermal neutron background of the form $\sqrt{E}\exp(-E/T)$ leads to a near-Gaussian shaped background in the relative velocity spectrum once detector acceptances and efficiences are taken into account [7]. Because of uncertainties in the background shape, we have modeled the background using a Gaussian line shape. The dashed line in Fig. 1 corresponds to the estimated background in this spectrum.

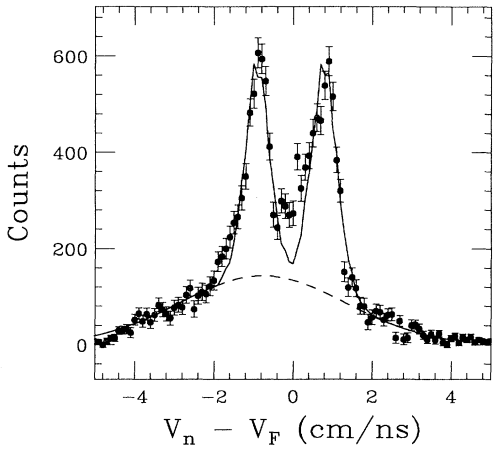


FIG. 1. The relative velocity spectrum for $n$+$^6$He coincidence events. The dashed line shows the estimated background and the solid line is a result of the simulated decay of ground state $^7$He.

A Monte Carlo program was written in order to compare the measured $n$+$^6$He relative velocity spectrum to the distribution expected from the decay of $^7$He. The program used energy and angular distributions for the primary $^7$He fragments as predicted by fragmentation systematics [9], and an isotropic $^7$He center-of-mass decay distribution to simulate the observed relative velocity spectrum. Detector acceptances and efficiencies were incorporated into the simulation, as was the experimental time resolution. Neutron detector energy-dependent efficiencies were calculated with the code KSUEFF [10]. Coulomb distortion of the relative velocity, which should be negligible in this low $Z$ reaction, was not included. The solid line in Fig. 1 shows the calculated spectrum for the $^7$He decay using a Breit-Wigner line shape of the form [11]

$$\frac{d\sigma}{dE} \propto \frac{\Gamma(E)}{(E-E_r)^2 + \frac{1}{4}[\Gamma(E)]}^2, \tag{1}$$

where $\Gamma(E) = \frac{P_l(E)}{P_l(E_r)}\Gamma_0$, $P_l(E)$ is the $l$-dependent neutron penetrability function, $E_r = 450$ keV, $\Gamma_0 = 160$ keV, and $l = 1$. This calculation, which was normalized to the data, reproduces the data rather well. The fit can be improved by modifying the decay parameters within their known uncertainties. The collinear detection geometry is found to be particularly sensitive to the low energy part of the decay line shape because of the high coincidence detection efficiency for low relative-energy events. On the other hand, this geometry is insensitive to nuclear alignment effects in the fragmentation reaction [12], because the coincidence events correspond only to decays very near 0° and 180° with respect to the beam axis. Furthermore, the dependency on the energy and angular distribution of the primary $^7$He fragment is rather weak.

Figures 2 and 3 show the relative velocity spectrum for the $n$+$^9$Li coincidence events. The data are dominated by a single peak near 0 cm/ns and the estimated background is shown by the dotted line. For $^{10}$Li, the

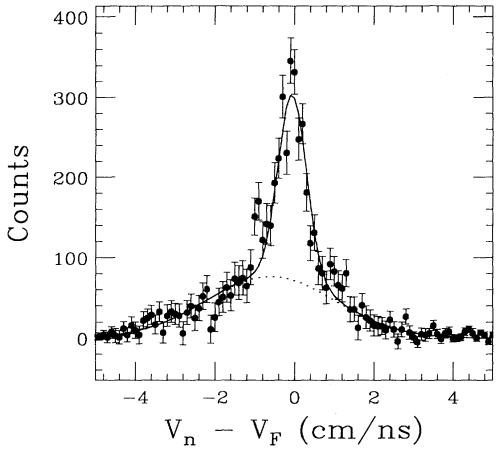


FIG. 2. The relative velocity spectrum for $n$+$^9$Li coincidence events. The dotted line shows the estimated background and the solid line shows the calculated spectrum for an $l = 1$ decay with $E_r = 50$ keV and $\Gamma_0 = 100$ keV.

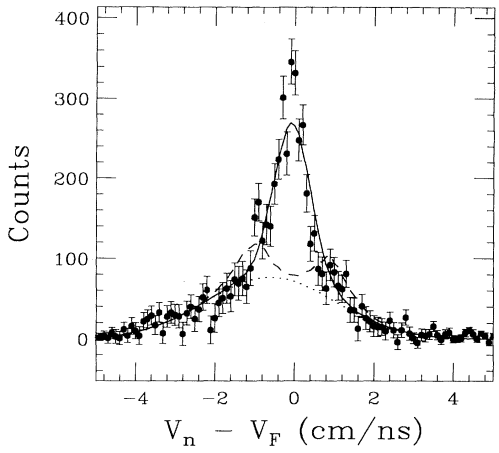


FIG. 3. The relative velocity spectrum for $n$+$^9$Li coincidence events. The dotted line shows the estimated background and the solid line is a result of the simulated decay of the $^{10}$Li ground state reported by Amelin *et al.* [4]. The dashed line is a result of a calculation for the $^{10}$Li state reported by Wilcox *et al.* [3], assuming $p$-wave emission.

most likely shell model configuration of the ground state involves a $1p$ or $2s$ valence neutron surrounding a $^9$Li core. Therefore, we considered decay line shapes associated with $l = 0$ or $l = 1$ neutron emission. For $p$-wave emission, a resonance energy of $E_r < 200$ keV is required for $\Gamma_0 < 500$ keV to produce a central peak in the calculation similar to the one observed in the data. (We use a $\chi^2_\nu < 2.0$ test when comparing the calculated and measured relative velocity spectra in the relative velocity range from $-4$ cm/ns to 4 cm/ns to establish our limits.) For 500 keV $< \Gamma_0 <$ 1500 keV the limit is $E_r < 300$ keV. As an example, the solid line in Fig. 2 shows the result of a calculation for $E_r = 50$ keV and $\Gamma_0 = 100$ keV which compares well with the data. Increasing $E_r$ widens the peak until the forward and backwards emission components of the decay are distinguishable (as in the $^7$He case). Increasing $\Gamma_0$ also widens the central peak. A similar result is obtained if we consider $s$-wave states although the limits on $E_r$ are less rigid because the $l = 0$ penetrability function does not suppress low-energy neutron emission as strongly. A resonance energy of $E_r < 300$ keV is needed for $\Gamma_0 < 500$ keV and the limit increases to $E_r < 450$ keV if 500 keV $< \Gamma_0 <$ 1500 keV. The solid line in Fig. 3 shows the calculated spectrum for $E_r = 150$ keV, the value reported by Amelin *et al.* [4], and $\Gamma_0 = 400$ keV corresponding to their upper limit. These parameters are consistent with the limits established in this work. On the other hand, the dashed line in Fig. 3 corresponds to the calculated spectrum for the $E_r = 800$ keV ($\Gamma_0 = 1.2$ MeV) state of Wilcox *et al.* [3] assuming a $p$-wave outgoing neutron (see discussion below) arbitrarily normalized to the data. There may be evidence for this state in the data near $\pm 1$ cm/ns, but this resonance cannot account for the large central peak in the data.

In contrast with the transfer reactions of Refs. [3, 5, 6] where one measures the energy of a resonance state directly, the SNDS method only determines the relative energy between decay products. Since $^9$Li has, in addition to the ground state, one particle-bound excited state at $E_x = 2.69$ MeV [8], it is not possible to distinguish whether the observed low-energy neutron decay populated the ground state or first excited state of $^9$Li. If the decay was to the ground state, the parent state would represent the ground state of $^{10}$Li consistent with the results of Amelin *et al.* [4], but with an energy significantly lower than the state reported by Wilcox *et al.* [3] or the state(s) seen in the other transfer data [5, 6]. It has been argued by Barker and Hickey [13] that the state seen by Wilcox *et al.* [3] was in fact an excited state of $^{10}$Li corresponding to the $[\pi\ 1p_{\frac{3}{2}} \otimes \nu\ 1p_{\frac{1}{2}}]$ shell model configuration and that the actual ground state lies approximately 800 keV lower, corresponding to a $[\pi\ 1p_{\frac{3}{2}} \otimes \nu\ 2s_{\frac{1}{2}}]$ configuration. This argument was based upon the non-normal parity of the $^{11}$Be ground state understood in terms of a $^{10}$Be core + $2s$ neutron and evidence that the lowest $T = 2$ state of $^{10}$Be was associated with an $s$-wave neutron [14]. It is conceivable that the observed state in the present work, as well as the pion absorption data, represent this $s$-wave ground state which may not have been seen in the transfer reactions of Refs. [3, 5, 6] if they preferentially populate $p$-wave states. On the other hand if the observed decay populates the first excited state of $^9$Li, it would be the first report of an excited state in $^{10}$Li in the relatively high excitation energy range of $E_x \approx 2.5$ MeV (the effect of the subsequent $\gamma$-ray decay of the $^9$Li nucleus on the relative velocity spectrum is negligible in our data). One possible configuration for such a state would be a $^9$Li core excited into its 2.69 MeV state with a $p$-wave valence neutron [15]. In the case of a high $E_x$ state in $^{10}$Li, it is energetically possible to decay to both the ground and first excited states of $^9$Li and the assumed line shape of Eq. (1) would need to be modified for a complete analysis.

In summary, we employed the method of sequential neutron decay spectroscopy at 0° to study neutron-unstable fragmentation products and observed a $^{10}$Li state which decays by the emission of a low-energy neutron. This state is consistent with the ground state reported by Amelin *et al.* [4], but the present results do not allow us to conclude that it is the ground state since it could also be an excited state in $^{10}$Li at $E_x \approx 2.5$ MeV.

We acknowledge helpful discussions with Alex Brown and support from the NSF through Grant No. PHY92-14992.

[1] H. Esbensen and G. F. Bertsch, Phys. Rev. C **46**, 1552 (1992). See also G. F. Bertsch and H. Esbensen, Ann. Phys. (N.Y.) **209**, 327 (1991).
[2] J. M. Bang and I. J. Thompson, Phys. Lett. B **279**, 201 (1992).
[3] K. H. Wilcox, R. B. Weisenmiller, G. J. Wozniak, N. A. Jelley, D. Ashery, and J. Cerny, Phys. Lett. **59B**, 142 (1975).
[4] A. I. Amelin, M. G. Gornov, Yu. B. Gurov, A. L. Ilín, P. V. Morokhov, V. A. Pechkurov, V. I. Savelév, F. M. Sergeev, S. A. Smirnov, B. A. Chernyshev, R. R. Shafigullin, and A. V. Shishkov, Yad. Fiz. **52**, 1231 (1990) [Sov. J. Nucl. Phys. **52**, 782 (1990)].
[5] H. G. Bohlen, B. Gebauer, M. von Lucke-Petsch, W. von Oertzen, A. N. Ostrowski, M. Wilpert, Th. Wilpert, H. Lenske, D. V. Alexandrov, A. S. Demyanov, E. Nikolskii, A. A. Korsheninnikov, A. A. Ogloblin, R. Kalpakchieva, Y. E. Penionzhkevich, and S. Piskor, Z. Phys. A **344**, 381 (1993).
[6] B. M. Young (private communication).
[7] F. Deak, A. Kiss, Z. Seres, G. Caskey, A. Galonsky, and B. Remington, Nucl. Instrum. Methods A **258**, 67 (1987).
[8] F. Ajzenberg-Selove, Nucl. Phys. **A490**, 1 (1988).
[9] J. A. Winger, B. M. Sherrill, and D. J. Morrissey, Nucl. Instrum. Methods B **70**, 380 (1992).
[10] R. A. Cecil, B. D. Anderson, and R. Madey, Nucl. Instrum. Methods **161**, 439 (1979).
[11] A. M. Lane and R. G. Thomas, Rev. Mod. Phys. **30**, 257 (1958). See Sec. XII.3.
[12] K. Asahi, M. Ishihara, T. Ichihara, M. Fukuda, T. Kubo, Y. Gono, A. C. Mueller, R. Anne, D. Bazin, D. Guillemaud-Mueller, R. Bimbot, W. D. Schmidt-Ott, and J. Kasagi, Phys. Rev. C **43**, 456 (1991).
[13] F. C. Barker and G. T. Hickey, J. Phys. G **3**, L23 (1977).
[14] S. N. Abramovich, A. I. Baz, and B. Ya. Guzhovskii, Yad. Fiz. **32**, 402 (1980) [Sov. J. Nucl. Phys. **32**, 208 (1980)].
[15] H. Esbensen (private communication).